

Generalized Spectral Performance Evaluation of Multijunction Solar Cells Using a Multicore, Parallelized Version of SMARTS

Joachim Jaus¹ & Christian A. Gueymard²

¹ Black Photon Instruments GmbH, Emmy-Noether-str. 2, 79110 Freiburg, Germany

² Solar Consulting Services, P.O. Box 392, Colebrook, NH 03576, USA

Abstract: The spectral composition of sunlight is subjected to constant changes due to variations in atmospheric conditions and varying path length of the sunrays through the earth's atmosphere ("air mass"). In this paper, we analyze the spectral direct irradiance based on the aerosol data from the AERONET ground sunphotometer network. Using a high-performance version of the simulation software SMARTS, the spectral irradiance is studied for 379 sites distributed worldwide. These calculations find particular application in concentrating photovoltaic power plants that use high-efficiency multijunction solar cells. To demonstrate the usage of the calculated spectra, the effects on the current balance for some cell designs available from the industry or research laboratories are calculated and compared to those under the reference spectrum AM1.5d from ASTM G173.

Keywords: Spectral performance, SMARTS, spectral irradiation, multijunction, current balance

PACS: 42.68.Jg, 42.79.Ek, 72.40.+w, 72.80.Ey

INTRODUCTION

Multijunction (MJ) solar cells are frequently used in CPV modules today. The solar spectrum has a significant influence on the performance of this kind of high-efficiency solar cell. The performance of MJ solar cells is commonly measured under a reference spectrum such as AM1.5d from ASTM G173. However, outdoor operating conditions can differ significantly from this spectrum. In this contribution, we analyze the spectral performance of some MJ solar cells that are currently on the market or under development, for a variety of atmospheric conditions.

METHODOLOGY

The NASA-operated AERONET network of ground sunphotometers offers quality-controlled, long-term measurements from over 600 stations over the world. Aerosol optical depth (AOD) and precipitable water (PW) data are derived from such measurements roughly every 15 minutes, when the sun is not obscured by clouds.

The SMARTS spectral radiative code [1, 2] accepts these atmospheric variables as inputs to simulate solar spectra. Based on these locally-defined and temporarily-variable solar spectra and the quantum efficiency (QE) of the subcells of each MJ solar cell under scrutiny, the subcell current densities and the resulting overall current density can be calculated and compared to the current density generated under reference (fixed) conditions.

To generate many spectra at many sites, we developed a fast, parallelized version of SMARTS that distributes the computation load to all sub-cores of multiprocessing architectures. We also developed means for automatic post-processing of the spectral data in order to facilitate simultaneous current calculations for a large set of solar cells.

AERONET SITE PROCESSING

The favorable time resolution of the AERONET database allows detailed and highly resolved spectral simulations. These can be used to determine which of various possible spectral effects have a real impact on the power generation of a CPV power plant, and which ones have no significant impact.

This work is based on AERONET atmospheric measurements as of March 17, 2012 (available at <http://aeronet.gsfc.nasa.gov>). At that date, the database contained data from 612 sites. At some sites, the atmospheric measurements had only been conducted for a few days only, resulting in a small number of data points. As we are looking for measurements that cover a significant period, those short-term measurement campaigns were filtered out by excluding all sites with less than 1000 measurements. The remainder still contains some sites that provided measurements during only a few weeks or months, and therefore are not necessarily representative of the seasonal evolution at such sites. The approach used here is to pool the data from all AERONET sites of significance. This guarantees that the seasonal differences of singular sites are leveled out in the entirety of the whole dataset.

The inputs used for our spectral calculations are: the AOD at 500 nm ("AOD"), precipitable water ("PW"), solar zenith angle ("SZA"), and the Ångström exponent ("Alpha"). Not all sites in the AERONET database contain measured data for each of these variables. To select only sites that contain valid information for all of them, a program in the python programming language has been written to scan through the whole dataset. Using this program, a reduced set of 379 sites with more than 1000 instances of valid AOD, PW, SZA, and Alpha variables has been identified.

The program is also able to generate histograms of each atmospheric variable for any single site, and for the entire dataset assembled from all sites as well. The first type of histogram is useful for a quick visual screening, whereas the latter type (as shown in Fig. 1) provides an impression of the worldwide distribution of these variables.

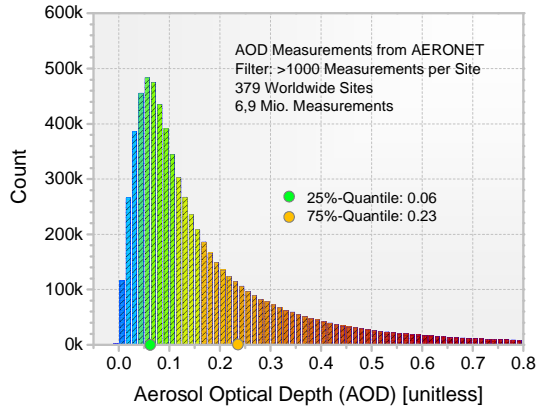


Figure 1: Histogram representation of AOD data for 379 worldwide distributed AERONET sites.

From the histogram representation, a lognormal distribution of AOD values can be observed. A similar histogram representation can also be calculated for PW and the Ångström exponent (Fig. 2).

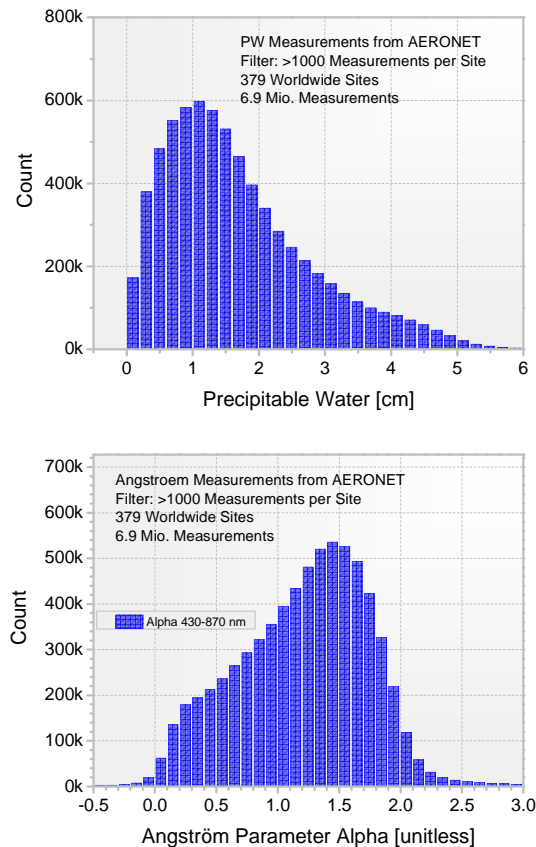


Figure 2: Frequency distributions of PW and Ångström exponent, yielding 0.85/2.27 cm and 0.84/1.60 for the 25/75% quartiles of PW and Alpha, respectively.

Histogram representations can also be obtained for air mass. However, due to the widely different site latitudes, they are of limited interest.

CALCULATION OF SPECTRA

Based on the AOD/PW/AM/Alpha variables, the direct normal spectral irradiance can be calculated using the high-performance version of SMARTS described above. For the 379 AERONET sites with significant data series, a total of 6.9 million spectra can be evaluated. Due to limitations in the AERONET algorithms, none of these spectra are for low-sun conditions. This translates into an effective maximum air mass of 7.

Parameters used in SMARTS

The SMARTS model makes heavy use of input and output files that it reads and writes from/to the computer’s hard disk. AOD and PW that have been extracted from the AERONET database are used here with normally no alteration. AOD values that are either negative or >15 have been excluded since they are not physical and would trigger error messages in SMARTS. Only a single Alpha value (from “440-870Ångstrom” in AERONET’s nomenclature) has been used for both the alpha1 and alpha2 values required by SMARTS, since this single Alpha is closer to the original Ångström approach, and less prone to measurement errors of small-band determination of the variation of AOD with wavelength. The SZA values provided by AERONET are used by SMARTS to calculate the corresponding air mass (“AM”). The elevation of each AERONET site has also been used as a direct input to SMARTS to evaluate the corresponding station pressure.

Statistical Representation of Calculated Spectra

To decrease the calculation time, the initial number of 6.9 million possible spectra has been reduced to 37,900 by randomly selecting only a fraction of the measured parameter sets in the AERONET database. We experimented with various numbers of sites and number of samples per sites. We found that the results of our calculations became stable within less than 0.1% when using 100 AOD/PW/AM/Alpha combinations per site.

When many thousand spectra are calculated, it is desirable to condense this information to make it manageable. Based on the SMARTS inputs described above, a statistical representation of the calculated spectra can be calculated, as shown in Fig. 3.

To obtain the summary results shown in Fig. 3, the calculated spectra have been aggregated in bins of 50 nm width. Within each bin, the spectral irradiances have been summed up. Then, a probability

function has been calculated to reveal the quintiles Q1/5 to Q5/5. In Fig. 3, the top of the bar columns indicate the spectral irradiance of Q1 to Q5, depending on the indicated color code. The star near the top of each bar column indicates the reference irradiance, per ASTM G173.

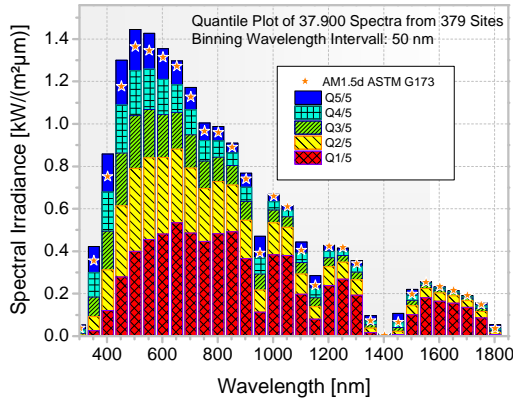


Figure 3: Spectrally binned representation of the spectra calculated for 379 sites based on 100 cases per site.

As can be seen in Fig. 3, a maximum spectral irradiance around 500 nm can be noticed, followed by a steep drop beyond 650 nm. This is true for both the reference spectrum and quintile 5. In the lower quintiles, the maximum shifts more and more to longer wavelengths, with a much less steep drop between 500 and 900 nm. This indicates a significant redshift of the spectrum for all quintiles other than 5, compared to the reference spectrum.

Spectral Performance of Multijunction Solar Cells

From the calculation of the subcell currents for each spectrum, the magnitude of the current losses or gains caused by spectral variations can be derived. The QEs of the multijunction cells examined in this work are plotted in Fig. 4.

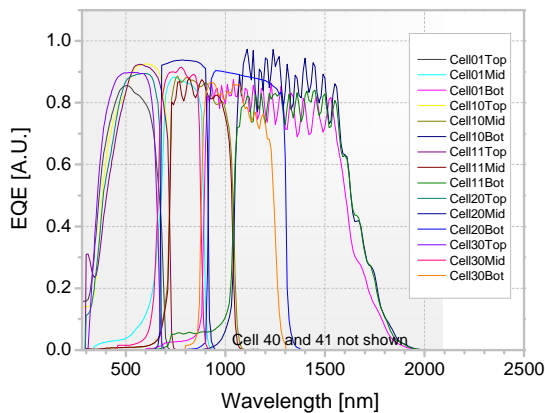


Figure 4: External QE for the seven cells used in this study. Three have been supplied by cell manufacturers, and four by research institutes.

An important aspect of MJ solar cells is the determination of the spectral performance, which basically describes their robustness vis-a-vis spectral changes in the incident irradiance. As a measure of this spectral performance, the short-circuit current (I_{SC}) of each MJ cell has been calculated by combining its spectral response (derived from its QE) and the SMARTS-derived spectra, one at a time. This is a simpler approach for cell modeling than the frequently used 1-diode models, or than more rigorous semiconductor simulation models (e.g., [3-5]). However, as shown in [3], the short-circuit current gives a reasonably good representation of the cell performance at operating conditions. To complement our approach, the additional effects of the fill factor, open circuit voltage, temperature, actual concentration, partial cell shading, spectral transmittance of the concentrator, etc., should be included to obtain a complete and realistic energy output analysis.

To determine the spectral performance, an I_{SC} -based Spectral Performance parameter, ISP , is obtained from Eq. (1):

$$ISP = \frac{\frac{\sum_{i=1}^N \min[\int SR_{Top,Mid,Bot}(\lambda) G_i(\lambda) d\lambda]}{\sum_{i=1}^N \int G_i(\lambda) d\lambda}}{\min[\int SR_{Top,Mid,Bot}(\lambda) G_{AM1.5d}(\lambda) d\lambda]} \quad (1)$$

with G_i : Spectral irradiance of Spectrum i
 N : Number of Spectra
 $G_{AM1.5d}$: AM1.5d ASTM G173.

The results of these calculations are summarized in Fig. 5.

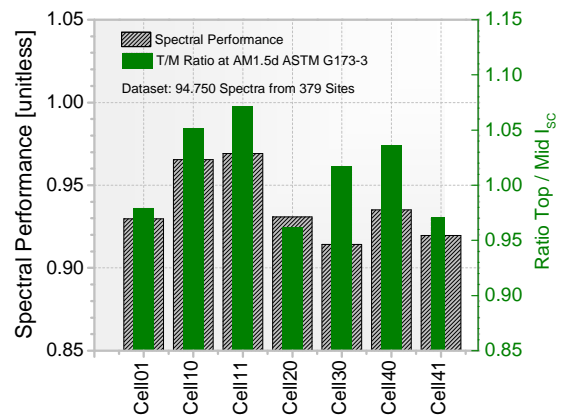


Figure 5: I_{SC} -based Spectral Performance Factor ISP as calculated with Eq. (1). The ratio of the I_{SC} at reference conditions (AM1.5d ASTM G173) of the top and middle cells are also plotted with the smaller bars.

As can be seen in Fig. 5, ISP varies between 0.93 and 0.97 for the seven cells analyzed here. These remarkably high values suggest that MJ cells do perform well under the very diverse conditions of the large set of sites used in the present analysis and that a 4th junction may still perform reasonably well.

The remaining difference between the cells indicates that the performance can still be optimized using spectral calculations as presented in this work.

Currently, a common design method is to optimize the subcell currents in order to achieve current matching at reference conditions. As can be seen in the comparison to the I_{SC} -ratio of the top and middle cells at reference conditions plotted in Fig. 5, the correlation between results of the two methods is only weak. (see e.g. Cell20 vs. Cell30). It is therefore beneficial to include detailed spectral performance calculations early in the design phase of a cell to achieve the best possible spectral performance.

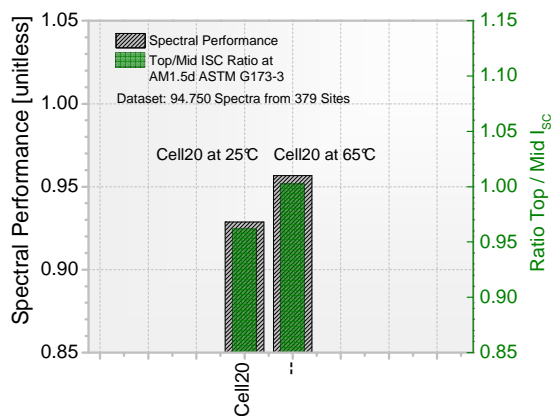


Figure 6: Influence of cell temperature on spectral performance. ISP is calculated for cell 20 using its spectral response at 25°C and 65°C.

As can be seen in Fig. 6, the cell's spectral performance is affected by the operating temperature, since the bandgap of the subcells shifts towards higher wavelengths with increasing temperature. Using SR data simulated or modeled at different temperatures, such temperature effects can be conveniently studied with our model. A dataset including ambient air temperatures with the same time and geographical resolution as the AOD/PW/AM/Alpha measurements from AERONET would be needed for such a purpose. This is possible at those AERONET sites that are collocated with other meteorological stations, but such occurrences are rare in the world, unfortunately.

When AOD increases, the spectrum is strongly red-shifted, while the corresponding broadband irradiance (direct normal irradiance, DNI) concomitantly decreases. Our intermediate calculations show that, among all the atmospheric variables studied here, AOD has the strongest effect on ISP . An increasing air mass also red-shifts the spectrum, but air mass is a pure function of SZA, so that sites at the same latitude experience the same mean air mass. Conversely, they may experience very different aerosol conditions, depending on elevation, proximity from aerosol sources, etc. A more detailed study on the effect of AOD on ISP is therefore desirable.

SUMMARY AND CONCLUSION

AERONET provides a high-quality database for the atmospheric variables that are necessary to evaluate the performance of MJ solar cells under diverse spectral conditions at any location in the world. To calculate the spectral irradiance, a high-performance version of SMARTS has been developed. To cope with the large amount of datasets available in the AERONET database, a random selection process has been devised to keep only 100 data point combinations per site. Spectral binning techniques are used to visualize the large number of spectra thus generated. The cumulative distributions based on 379 sites and 37,900 direct spectra show that the worldwide they are statistically more red-rich than the reference spectrum ASTM G173.

To evaluate each of seven current MJ cell's spectral performance, a simple short-circuit current-based approach is used. A world-average spectral performance factor between 0.93 and 0.97 is obtained. Our results indicate that further optimization of MJ cells and systems is possible, e.g. by fine-tuning the band gaps of the subcells to make them current matched under realistic spectral conditions.

ACKNOWLEDGMENTS

The authors express their gratitude to Brent Holben and his team for supplying the AERONET data. The support of David Giles at NASA GSFC for all database-related questions has been particularly helpful. The authors also thank the research institutes and cell manufacturers that supplied spectral response data. This work has been partially funded by the German Environment Foundation (DBU) under contract number AZ29371, which is highly appreciated.

7. REFERENCES

- [1] C. Gueymard, "Parameterized transmittance model for direct beam and circumsolar spectral irradiance," *Solar Energy*, vol. 71, no. 5, pp. 325-346, Nov. 2001.
- [2] C. Gueymard, "SMARTS2, a simple model of the atmospheric radiative transfer of sunshine: algorithms and performance assessment," Report FSEC-PF-270-95. Florida Solar Energy Center, 1995.
- [3] S. P. Philipps et al., "Energy harvesting efficiency of III-V triple-junction concentrator solar cells under realistic spectral conditions," *Solar Energy Materials and Solar Cells*, vol. 94, no. 5, pp. 869-877, May. 2010.
- [4] D. J. Friedman and S. R. Kurtz, "Breakeven Criteria for the GaInNAs junction in KaInP-GaAs-GaInNAs-Ge Four-junction Solar Cells," vol. 14, pp. 1-14, 2002.
- [5] S. Nann and K. Emery, "Spectral Effects on PV-device rating," *Solar Energy Materials and Solar Cells*, vol. 27, pp. 189-216, 1992.